

A FEATURE BASED APPROACH TO HIGH PRESSURE COMPRESSOR PRELIMINARY DESIGN FOR CIVIL AIRCRAFT PROPULSION SYSTEMS

S. Bretschneider, S. Staudacher
Institute of Aircraft Propulsion Systems
Stuttgart University
Pfaffenwaldring 6, 70569 Stuttgart
Germany

OVERVIEW

This paper outlines a strategy to scale axial high pressure compressor components for civil aircraft engines in preliminary concept studies to achieve higher levels of component detailing. Features based on parts were developed and equipped with design-rules to maintain compatibility between detailed concepts. Examples are presented why such detailing level has become necessary. To show this goal a typical commercial compressor is deconstructed into a set of similar parts. From the similarity so called features or generalized parts are derived which have the capability of scaling themselves by physical design rules. The feature tree of the described axial compressor is presented. Also the design methodology of the single features is described. The compressor component is then reassembled by the application of the derived features and a generalized form of an axial high pressure compressor is generated. Finally results from the application of the model to known high pressure compressors are presented and discussed. Thus the paper shows how generalized design based on features can be used to achieve high levels of detail for compressor preliminary design. The advantage of the methods is that during the concept phase only little input data from performance calculation and design rules from knowledge based engineering are required.

NOMENCLATURE

C	Constant
E	Modulus of elasticity
FEM	Finite element methods
HPC	High pressure compressor
IGV	Inlet guide vane
m	Slope
n	Constant
PD	Preliminary design
r	Radius
SF	Safety factor
T	Temperature
ΔT	Delta temperature against reference
u	Displacement
α	Thermal expansion coefficient

ν	Poisson number
ρ	Density
σ	Stress
σ_y	Ultimate strength
σ_{avg}	Average tangential stress
σ_e	Equivalent stress
σ_y	Yield strength
ω	Rotational speed

1. INTRODUCTION

When looking at the overall development of preliminary design (PD) processes it is found that recent research aims to include a much broader field of topics into the investigation of new engine concepts than has been done in the past. The prediction of economic aspects of every engine study case has become a significant aspect in preliminary design. At very early stages new concepts are evaluated for their full life cycle costs, including topics such as maintenance or production cost. Also the growing impact of the ongoing discussion on how to tackle the world's climate problem pushes the aerospace industry into the challenge of finding more and more environmentally friendly engine concepts. Thus ecological questions are addressed as early as possible in the preliminary design stage trying to evaluate the environmental impact of studied concepts in a clearly economically orientated business world [1] [2]. Engine manufactures do also face a constant pressure to lower development times and costs, thus it becomes very clear that the availability of high quality preliminary design tools has become significantly more important.

When topics addressed in modern PD activities are investigated, it is clear that rather traditional PD tasks such as engine performance optimisation and weight prediction are no longer the final target but have developed more and more into necessary steps towards the evaluation of full life cycle costs including the engines ecological impact. Models which do address advanced PD topics such as production or maintenance cost are often only applicable when the detailed engine design already is known [3]. Since PD concept studies are aimed for finding the optimum solution out of thousands of possibilities this level of detail cannot be provided by the traditional design finding process because detailed design is time intensive work and usually comes in a later phase of the engine

development process when decisions from the preliminary design have already been made.

Thus the challenge arises to provide preliminary design with higher detail. The work presented in this paper does concentrate on the question whether the generation of a high pressure compressor PD tool is possible which does provide a detailed component on a rather generalized manner (instead of a optimized component design).

2. COMPRESSOR PRODUCT STRUCTURE

Over the last decades high pressure compressors have been developed to very high levels of sophistication leaving only little degrees of freedom left for improvement. Looking into the forward direction this fact challenges engineers harder to improve models and methods to push the boundaries even further. From the current PD view on what has been achieved over the last years it can be recognized that only very little changes in compressor product structure have been made over the last years. Not taking into account aerodynamic improvements, the introduction of Blisks and new materials have been major changes. High pressure compressors appear to be matured pieces of engineering. This level of consolidated component design and its continuity are the very basis of the methodology presented here.

When investigating existing axial HPC components one will find that all designs contain the same structure almost right from the very beginning. Axial compression is achieved by stacking a number of compressor stages. Each single stage itself is built from a rotor and a stator component. To contain the gas channel casings are added which give the shroud and hub walls for the stators. Rotors are structured in rotating blade rows which need to be supported by disks, and over the years only a limited number of connection strategies have been developed to attach the blade to the disk. For a conventional HPC design the disks are then connected by arms to form the high pressure shaft. Comparing the parts in the individual compressor stages the similarities in shape become very obvious. But not only the geometry is similar, also the underlying design methodology is equal and thus the observed geometrical similarities are a function of the same design algorithm using individual input data and stage dependent characteristics.

For the model presented here the full HPC component has been deconstructed into such similar parts. The parts themselves have then been developed into so called features. A feature represents a certain part of the compressor, e.g. a disk, which has been generalized in a manner that all designer and engine individual characteristics have been removed and only the pure basic-design features have remained. Further each feature was equipped with a suitable design algorithm. As a result the derived features have the capability of being automatically designed for a given set of individual input parameters. From such generalized features the HPC component is then reassembled by implementing the interaction between the self-designing features. Thus the achieved HPC component represents a generalized form of a detailed compressor design. The model provides not only weight data but also geometrical information on a level as it is necessary to run more sophisticated models

(as described earlier) and to start a detailed design process. The structure of the described compressor part similarities which is at the same time equal to the structure of the derived features are presented in Fig. (1).

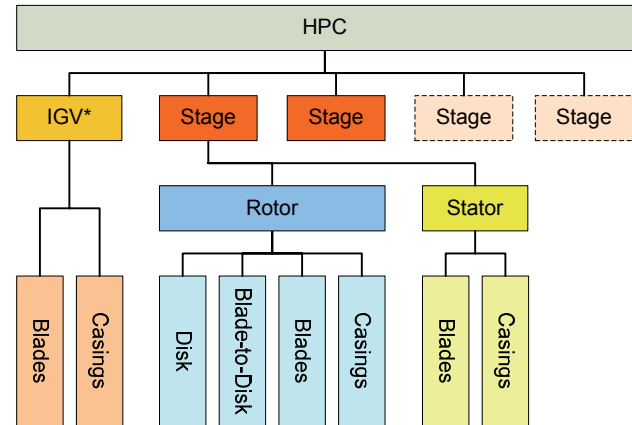


FIG 1. Feature structure of high pressure compressor * with optional inlet guide vane (IGV)

3. FEATURE DEFINITION

The features derived in the previous section have been implemented as independent models. Each is characterized by a generalized geometry definition. To determine the shape design methods based on physics are used. This enables design-ruled scaling instead of pure geometrical scaling. All features are integrated into a full component assembly taking into account all interdependencies of the individual features.

3.1. Model Input and Stage Definition

Input to the feature assembly is only based on performance data, such as compressor inlet flow condition, pressure ratio and efficiency. The number of stages and pressure ratios is derived from the input and built-in technology data and so the work load distribution is computed. An example distribution of pressure ratios over stages is shown in Fig. (2). Now the necessary number of stage features can be allocated and values are assigned to perform the blades' flow angle computation and to generate the information necessary to perform the design of the blade features.

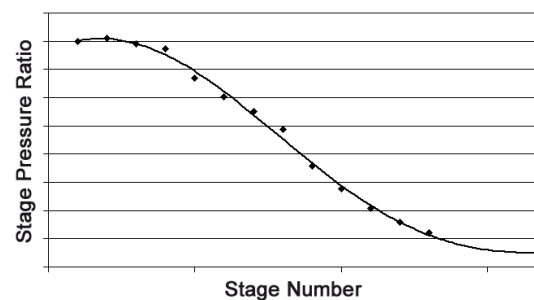


FIG 2. Pressure ratio distribution [4]

To provide quality thermodynamic computations a state of the art fluid model has been implemented. This type of fluid model is widely used also in performance calculations (similar as proposed by [5]). This also guarantees the comparability of the gas output values to the performance tool which has generated the overall input data.

3.2. Compressor Blading Feature

In traditional compressor preliminary design approaches blades are often simplified as flat plates which are characterized by a mean chord length, a mean blade height and an averaged blade thickness, e.g. see [6]. To get to the right numbers for these averaged values usually access to detailed design data or a data base is necessary. To avoid this problem a blading feature has been designed that derives blade shapes from flow angles and standard compressor profiles. Thus the goal of the blading methodology is not to generate an aerodynamically optimised set of blades. The aim is to obtain bladed rings that represent the mechanical form and behaviour of optimised blades without being computing-time intensive in calculation. This approach will of course not satisfy the aerodynamicists but will deliver rapid results in PD optimization and concept studies while still getting close to the real life part.

From the input a simple mean line design method is used to compute the flow angles at the mean diameter. Afterwards a vortex method [7] is applied to get the flow angles over the full radial expansion of the blade and so the typical twisted blade shape is achieved. Defining also the aspect ratio and blade's maximum thickness the blade shape is generated from a standard profile definition. An example of a rotor blade can be seen in Fig. (3). The full blade ring is finally obtained from simple circular replication of the blade shape.

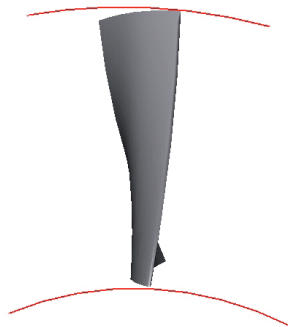


FIG 3. Front view on single rotor blade including sketched channel walls. [4]



FIG 4. Full blading result example [4]

The output information of each stage's previous blade row and the overall input from work and pressure distribution is used to derive each stage. The full compressor blading is then successively generated and iteratively solved for the specified output condition. The methodology of compressor blading has been developed and described by Jung [4].

3.3. Blade-to-Disk Connection Feature

After the definition of the compressor stages and blading has been performed a suitable disk design needs to be found including the connection of the blades to the disk. Following the approach from Armand [8] and Tong [9] shown in Fig (5), the disk is divided into two parts: a so called dead-load area which contains the blade foot and the corresponding support structure and the live disk which does carry the load imposed by the blades and the dead-weight section.

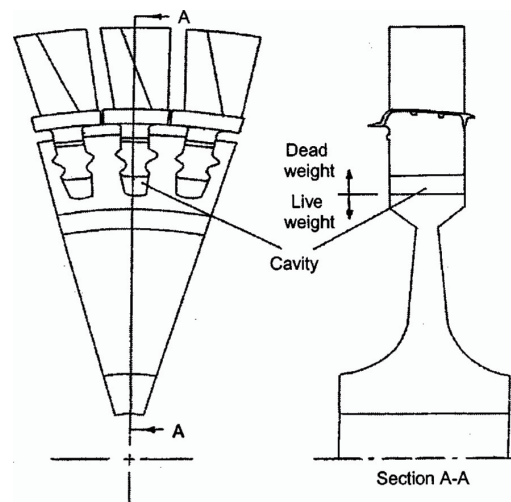


FIG 5. Blade to disk assembly [9]

The blade-to-disk feature designs the dead-load section which is ruled by the connection of the blades to the disk. Especially in compressor stages where the blades themselves have rather small weights, the impact of the chosen blade to disk connection type has a significant impact on the loads imposed on the live disk, which makes the investigation of the blade to disk connection a necessary question.

In current HPCs generally speaking four types of blade to disk connections are widely used:

- a) Circumferential dovetail type connections
- b) Axial dovetail type connections
- c) Axial fir-tree type connections
- d) Blistk type connections

Note that the last mentioned Blistk type connections are rather new compared to the other attachment strategies. Here the blades are mounted directly to the disk using manufacturing processes such as friction welding or even

the milling of a disk with blades from one single piece of pre-forged metal. Thus the disk-to-blade feature degenerates itself to a dummy feature without geometry when a Blisk type connection has been selected and the blades are directly mounted to the disk.

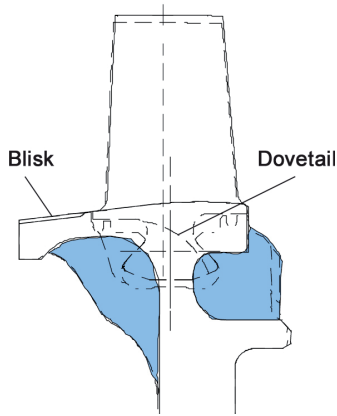


FIG 6. Example of a Blisk and a circumferential dovetail type blade-to-disk connection [10]

Circumferential dovetail type blade-to-disk connections are most often found in the rear stages of high pressure compressors where hub wall radii are usually larger than in the front stages but blade heights are significantly smaller while also having larger blade numbers. The stress scenario for the blade-to-disk connection is less critical and thus allows for the lighter and cheaper to manufacture circumferential dovetail connection.

Axial dovetail type connections become attractive when circumferential connections become overstressed. They do carry higher stresses but also imply a bigger dead-load to the disk which itself becomes heavier as a consequence. Thus the blade-to-disk feature switches to the axial dovetail solution when no feasible circumferential foot and tang connection can be found within the design constraints. As an extension of the axial dovetail type fir-tree connections are well known. Again they have the capability of attaching blades at higher stress levels to the disk but always come with increased loads on the supporting disks.

Since manufacturing such a connection is a very expensive procedure aerospace industry came up with standardized dovetail and fir-tree shapes. It is common practice for design engineer to only pick from a list of possible solutions instead of individually designing each blade-to-disk connection. This design methodology has also been chosen for the feature describing the real world. The feature selects the smallest and thus lightest possible solution from a table of blade roots. The design calculation is performed as proposed by Sawyer [11] and so at the same time the smallest possible stress scenario is achieved for the disk design.

3.4. Compressor Disk Feature

The disk feature is used to design the live section of the compressor disk as shown in Fig (5). The disk design algorithm itself is only dependant on the stresses and

dimensional results received from the blade-to-disk feature and on the general geometrical constraints set for compressor disks in the overall structure. Three common-known disk types used for typical turbomachinery disk shapes have been implemented as shown in Fig. (7).

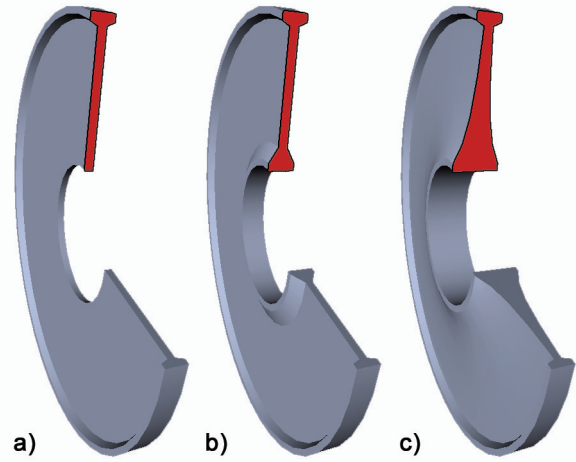


FIG 7. a) Ring disks, b) Web disks, c) Hyperbolic disks

All the dead-loads have already been calculated in the blade-to-disk feature and the stresses at the live disk rim are thus known and only the geometrical constraints and the bore diameter needs to be added to calculate the disk stresses. For the stress analysis an approach according to Tong et al. [8] [9] was used and extended. The assumptions made by this approach require the disk to be thin compared to its radial expansion. Only then the stresses can be reduced to the disks radial mean line. This assumption has been around in design theories for many years, e.g. [12] or [13], and was successfully used at the times where FEM calculations had not been come into practice yet. For the approach used the disk is represented by a large number of thin radial ring elements each having a linearly changing thickness. Each disk ring element is individually characterized by its linear thickness distribution

$$(1) \quad t = mr + n$$

where m is the slope and n a constant. The differential equation of equilibrium for such a rotating disk ring is given by [12] as

$$(2) \quad \frac{d}{dr}(tr\sigma_r) - t\sigma_\theta + t\rho\omega^2 r^2 = 0$$

where

$$(3) \quad \sigma_r = \frac{E}{1-\nu^2} \left[\frac{du}{dr} + \nu \frac{u}{r} - (1+\nu)\alpha\Delta T \right]$$

$$(4) \quad \sigma_\theta = \frac{E}{1-\nu^2} \left[\frac{u}{r} + \nu \frac{du}{dr} - (1+\nu)\alpha\Delta T \right]$$

are the tangential and radial stresses while u represents the displacement field of each disk element. To include the effect of varying temperatures over the disk a radial temperature field is prescribed also as a linear distribution

$$(5) \quad T = m_T r + n_T$$

or as given by Fourier's law [14]

$$(6) \quad T = T_{Bore} + \frac{T_{Rim} - T_{Bore}}{\ln\left(\frac{r_{Rim}}{r_{Bore}}\right)} \ln\left(\frac{r}{r_{Bore}}\right).$$

When setting a temperature field it is clear that most of the material characteristics will no longer be constant but will change as a function of temperature and thus also as a function of radius. Therefore, Armand's [8] approach was extended to also deal with the influence of material constant gradients over the disk radius, while assuming only the changes in density to be negligible small. When substituting the equations into Eq. (2) one single ordinary differential equation for the disk radial displacement field is obtained.

$$(7) \quad \frac{d^2u}{dr^2} + C_1 \frac{du}{dr} + C_2 u = C_3$$

with

$$(8) \quad C_1 = \frac{2mr + n}{mr^2 + nr} + \left[\frac{dE}{dr} \frac{1}{(1-\nu^2)} + \frac{2E}{\sqrt{1-\nu^2}} \frac{d\nu}{dr} \right] \frac{1-\nu^2}{E}$$

$$(9) \quad C_2 = -\frac{\nu}{r^2} - \frac{1}{r^2} + \frac{\nu}{r} C_1$$

$$(10) \quad C_3 = (1+\nu) \left[\alpha \frac{dT}{dr} + \Delta T \frac{d\alpha}{dr} + \alpha \left(C_1 - \frac{1}{r} \right) \Delta T \right] - \frac{1-\nu^2}{E} \rho \omega^2 r$$

Since all the material constants are known for each disk element Eq. (5) can be solved by common known numerical techniques as a boundary value problem. For this study a solving algorithm was implemented and the boundary conditions have been defined at the disk's rim and bore element. The bore boundary condition

$$(11) \quad \sigma_r = 0 \text{ at } r = r_{Bore}$$

is evaluated into

$$(12) \quad \frac{du}{dr} + \nu \frac{u}{r} - (1+\nu)\alpha\Delta T = 0.$$

The rim boundary condition is similar, except now a prescribed rim load needs to be met.

$$(13) \quad \sigma_r = \sigma_{Rim} \text{ at } r = r_{Rim}$$

gives

$$(14) \quad \frac{du}{dr} + \nu \frac{u}{r} \frac{(1-\nu^2)}{E} \sigma_{Rim} - (1+\nu)\alpha\Delta T = 0$$

where σ_{Rim} represents the average centrifugal stress at the live disk rim. According to Eq. (3) and (4) the computed displacement field also gives the stress field in the disk, which can be assessed to fulfil certain design criteria.

To derive the disk shape for given rim load and geometrical boundary conditions a design strategy similar to the one proposed by Tong [9] has been implemented. For all disks the outer rim dimensions and the shoulder are defined by input values from the results of the blade-to-disk feature and are thus kept constant in the disk shape definition.

Ring Disks: The web thickness is first set to the internal minimum value. Then the stress and displacement calculation is performed. If the design criteria is not fulfilled the web thickness is iteratively enlarged until the algorithm either finds a converged solution or concludes that no suitable design can be found within the defined boundary conditions.

Web and Hyperbolic Disks: Similar to the ring disk the disk configuration also starts with the minimum allowed web and bore thickness. Due to the increasing impact of weight added with raising radius the bore geometry parameters are increased first to find a feasible design solution. If the design criteria cannot be fulfilled further steps do increase the web thickness and later also the rim size of the bore section until a solution is found or the geometrical boundary conditions are met.

All strategies end in finding a solution, which will not be equal to a weight optimized one but will be close, or indicate that no suitable disk shape can be found within the boundary conditions.

The disk design criteria are defined by [9] as design margin

$$(15) \quad \frac{\sigma_y}{SF \cdot \sigma_e} - 1.0 > 0$$

and disk burst criteria

$$(16) \quad \frac{0.47\sigma_{ms}}{\sigma_{avg}} - 1.0 > 0.$$

3.5. Casing Features

The present version of the PD tool uses simple ring shapes to approximate compressor casing structures. An average thickness needs to be assumed for the casing structure to represent the overall weight impact. When looking at casing structures it can easily be seen, that the definition of the exact value for such an approximated averaged thickness is a very complex task in itself. Due to the complexity of the issue the findings of the current research in this field will be published in a subsequent paper.

4. RESULTS AND DISCUSSION

For this paper the derived model has been applied against known geometries. To study model results and behaviour the NASA E³ Engine HPC [15] and a theoretical reengineering of a 25000 lbf thrust class engine compressor [16] was used and promising results were archived. When comparing the achieved results with the data published for the NASA E³ engine the predicted general similarity can be observed.

A comparison of the flow channels can be seen in Fig. (8) and (9), note that the figures are not of the same scale. It can be seen that the mass flow conservation does result in almost the same flow channel shape. The observed

differences in compressor length result from the larger spacing between the individual blade rows.

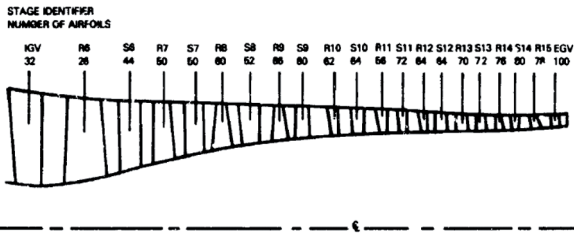


FIG 8. Flow channel of NASA E³ HPC engine from [15]



FIG 9. Flow channel feature-based generated HPC of NASA E³ engine

In general the model has the tendency to under-predict blade numbers especially in the rear stages. This is due to the used blade number estimation method taken from [13]. The general shape of the compressor blades do have similarities from the preliminary design point of view and are a valid representation of blade masses and inertia. Aerodynamically the blade sets will be completely different, but this was expected from the beginning. As mentioned earlier, the optimization of aerodynamics is not seen as part of this preliminary design activity.

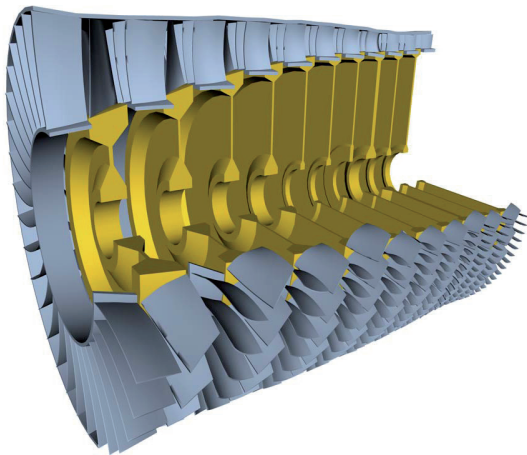


FIG 10. NASA E³ high pressure compressor with IGV

The disk design algorithm was proven to run fast and is stable with very satisfying results especially for thin disks as in the rear stages of the compressor. Disks with larger radius to thickness ratio do of course suffer from the simplification (thin disk assumption) of the disk stress theory and thus appear to have a too thin web section. In general the computed disks are thinner and therefore lighter than their real versions. This on one hand is an

error which is inherited by the described underestimation of the blade numbers causing too little load on the disks. On the other hand it strongly supports the idea of design-based scaling showing the targeted behaviour of reducing the disk size when removing blades. So the disk features do not only scale by shape but by load which is a clear advantage. Fig. (10) and (12) illustrate the described effect in the middle stages.

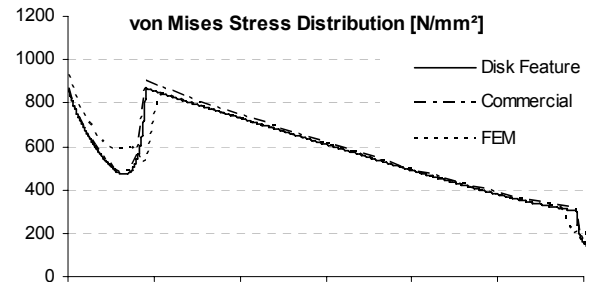
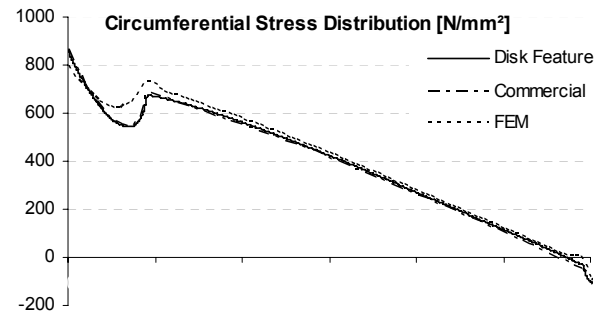
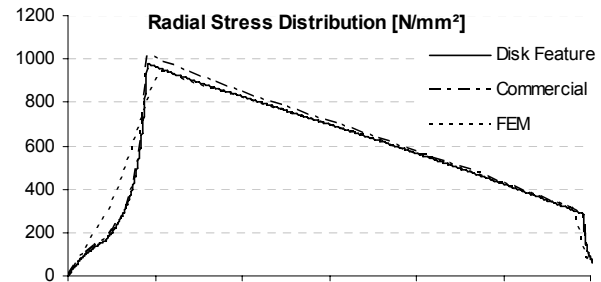
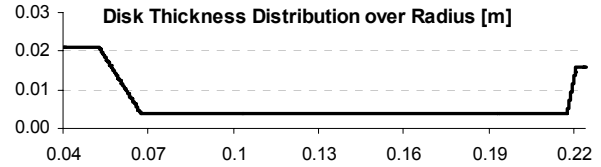


FIG 11. Example disk validation results

Since disks have a significant impact on the compressor weight estimation the extended stress calculation method was carefully validated. An example calculation is presented in Fig. (11). Here the used method was compared to a commercially available tool also referring to Tong's and Armand's approach and the same disk computed using FEM. Fig. (11) shows the radial mean line stress distribution for the FEM computed disk. All three computations show good agreement. Especially the stress peaks are well predicted by the non-FEM methods. Both non-FEM solutions do lie on the conservative side.

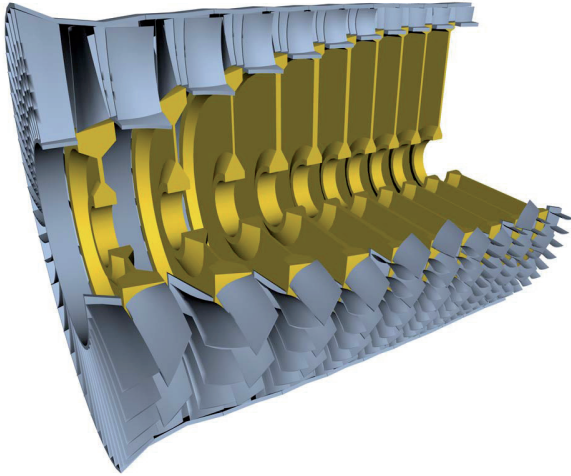


FIG 12. High pressure compressor including IGV of a 25000 lbf thrust class engine

The compressor generated for the 25000 lbf thrust class engine is shown in Fig. (12). Results achieved and also the observations made for model behaviour are equal to the already described ones. This underlines the comparability of the preliminary design approach and the consistency of the used design rules.

It is also worth to mention that the resulting data structure from the interdependency of all parameters and the feature interaction produces a very complex logical structure thus the advantage of using mainly analytical and text-book design methods becomes obvious. Simplification helps to understand the feature behaviour and also allows the engineer to understand the result although some of the received results do not yet have the quality as required for a final engine design.

5. SUMMARY

The question was raised if it is possible to build a generalized preliminary design model for high pressure compressors by creating design-ruled scalable features taking into account the maturity of compressor design technologies. Thus a feature structure for the compressor has been defined and the individual features were built. Features have been developed to represent blades, disks, blade-to-disk-connections and casings. The reassembly of the component then led to a complex system of interacting parameters and physical dependencies. When solving the model for two known geometries satisfactory results could be achieved. The results have been presented and discussed showing that design-based scaling does result in advanced capabilities for PD designers.

ACKNOWLEDGEMENTS

The model presented in this paper was implemented using the preliminary design software *Pacelab Suite V2.1* from *Pace Aerospace Engineering and Information Technology GmbH*. The authors wish to acknowledge the licence of software and the appreciated support of *Pace* as well as the fruitful discussions with company staff.

REFERENCES

- [1] Korsia, J.-J.; *Environmentally Friendly Aero Engine VITAL*; Invited lecture VII; 17th ISABE Conference, Munich, 2006
- [2] Bretschneider, S., Arago; *Architecture of a Techno-Economical and Environmental Risk Assessment Tool Using A Multi-Modular Build Approach*; ISABE2007-1103; Proceedings of ISABE Conference; Beijing; 2007
- [3] Arago, O.; Bretschneider, S.; Staudacher S.; *A Unit Cost Comparison Methodology for Turbofan Engines*; GT2007-27485; Proceedings of ASME Turbo Expo 2007; Power for Land, Sea and Air; May 14-17, Montreal, 2007
- [4] Jung, M.; *Erstellung eines Vorauslegungstools für die Beschaffung von axialen Hochdruckverdichtern für zivile Luftfahrtantriebe in der Entwicklungsumgebung PACELAB*; Studienarbeit, Institut für Luftfahrtantriebe, Universität Stuttgart; 2007
- [5] Munzberg, H.G.; Kurke, J.; *Gasturbinen Betriebsverhalten und Optimierung*; Springer Verlag; 1977
- [6] Kurzke, J; *Gasturb 11 Program Manual*, Version 11, 2007
- [7] Cumpsty, N.A.; *Compressor Aerodynamics*; Krieger Publishing Company; Second Edition; 2004
- [8] Armand, Sasan C. ; *Structural Optimization Methodology for Rotating Disks of Aircraft Engines*; NASA Technical Memorandum 4693, November 1995
- [9] Tong, Michael T.; Halliwell, Ian; Ghosn, Louis J.; *A Computer Code for Gas Turbine Engine Weight and Disk Life Estimation*; Journal of Engineering for Gas Turbines and Power, Vol. 126, 2004
- [10] Kappmayer, G.; *Blisk Technologie in modernen zivilen Flugzeugtriebwerken am Beispiel des Rolls-Royce BR715 Triebwerkes*; DGLR-JT2001-104; Deutscher Luft- und Raumfahrt Kongress, 2001
- [11] Sawyer, John W.; *Sawyer's Gas Turbine Engineering Handbook*, Third Edition, Volume 1, Turbomachinery International Publications, Norwalk, USA, 1985
- [12] Traupel, Walter; *Thermische Turbomaschinen – Zweiter Band*; Springer-Verlag; Berlin/Göttingen /Heidelberg; 1960
- [13] Bohl, Willi; *Strömungsmaschinen 2 – Berechnung und Kalkulation*; 7. aktualisierte Ausgabe, Vogel-Buchverlag; 2005
- [14] Holman, J.P.; *Heat Transfer*; Seventh Edition, McGraw-Hill, New York, 1990
- [15] Bisset, J.; Howe, D.; *Energy Efficient Engine Flight Propulsion System – Preliminary Analysis and Design Report*; NASA CR-174701; 1983
- [16] Schlüter, R.; *Konstruktive Auslegung des Hochdruckverdichters von zivilen Flugtriebwerken der 25000lbf Schubklasse*; Diplomarbeit; Institut für Luftfahrtantriebe, Universität Stuttgart; 2006